

UNCLASSIFIED

AD 420647

DEFENSE DOCUMENTATION CENTER

FOR

SCIENTIFIC AND TECHNICAL INFORMATION

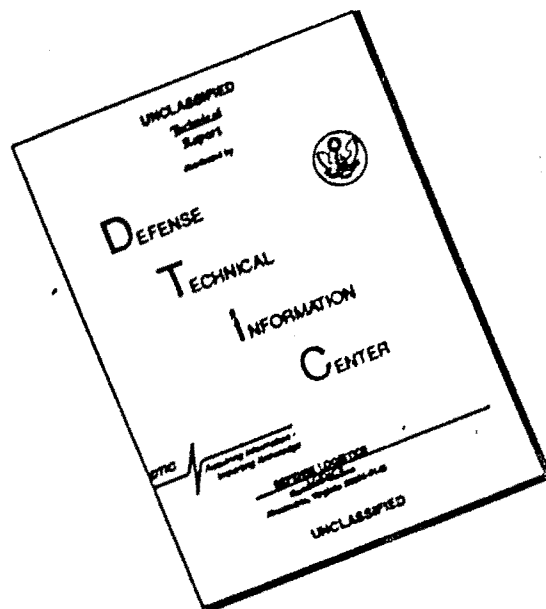
CAMERON STATION, ALEXANDRIA, VIRGINIA



UNCLASSIFIED

NOTICE: When government or other drawings, specifications or other data are used for any purpose other than in connection with a definitely related government procurement operation, the U. S. Government thereby incurs no responsibility, nor any obligation whatsoever; and the fact that the Government may have formulated, furnished, or in any way supplied the said drawings, specifications, or other data is not to be regarded by implication or otherwise as in any manner licensing the holder or any other person or corporation, or conveying any rights or permission to manufacture, use or sell any patented invention that may in any way be related thereto.

# DISCLAIMER NOTICE



THIS DOCUMENT IS BEST QUALITY AVAILABLE. THE COPY FURNISHED TO DTIC CONTAINED A SIGNIFICANT NUMBER OF PAGES WHICH DO NOT REPRODUCE LEGIBLY.

11ato

830200

NO. 420647

Technical Report No. 140

FILE COPY

On the Influence of Viscoelastic  
Compressibility in Stress  
Analysis,

by N. C. Huang, E. H. Lee  
and T. G. Rogers,

August 1963

Prepared under  
Office of Naval Research  
Contract Nonr 225(69)  
Contract Report No. 1

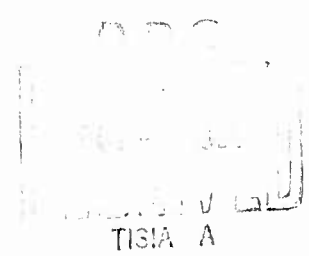
420647



Division of  
ENGINEERING  
MECHANICS



STANFORD  
UNIVERSITY



WJB

ON THE INFLUENCE OF VISCOELASTIC  
COMPRESSIBILITY IN STRESS ANALYSIS\*

By N.C. Huang, E.H. Lee and T.G. Rogers

Stanford University

Abstract

Almost all the solutions in the literature of viscoelastic stress analysis have dealt with materials which exhibit viscoelastic behavior in shear but are incompressible or elastic in dilatation. This has been influenced in part by the fact that accurate measurement of viscoelastic characteristics in dilatation are difficult to make, and only now are preliminary results becoming available. Since more precise measurements of dilatational response can be expected, certain solutions of viscoelastic stress analysis problems are presented to illustrate the convenience of utilizing measured relaxation moduli in dilatation as well as shear in evaluating stress distributions. Examples for cylindrical boundaries are given. These solutions are also useful in suggesting experimental configurations from which the relaxation modulus in dilatation can be deduced mathematically while avoiding the difficulties of direct measurement by surrounding a specimen with fluid under pressure. Metal casings can be incorporated

---

\* The results communicated in this report were obtained in the course of an investigation conducted under Contract Nonr-225(69) by Stanford University with the Office of Naval Research, Washington, D. C. Reproduction in whole or in part is permitted for any purpose of the United States Government. This work is to be presented at the Fourth International Congress on Rheology, at Brown University, Providence, R. I., August 1965.

ON THE INFLUENCE OF VISCOELASTIC  
COMPRESSIBILITY IN STRESS ANALYSIS\*

By N.C. Huang, E.H. Lee and T.G. Rogers

Stanford University

Abstract

Almost all the solutions in the literature of viscoelastic stress analysis have dealt with materials which exhibit viscoelastic behavior in shear but are incompressible or elastic in dilatation. This has been influenced in part by the fact that accurate measurement of viscoelastic characteristics in dilatation are difficult to make, and only now are preliminary results becoming available. Since more precise measurements of dilatational response can be expected, certain solutions of viscoelastic stress analysis problems are presented to illustrate the convenience of utilizing measured relaxation moduli in dilatation as well as shear in evaluating stress distributions. Examples for cylindrical boundaries are given. These solutions are also useful in suggesting experimental configurations from which the relaxation modulus in dilatation can be deduced mathematically while avoiding the difficulties of direct measurement by surrounding a specimen with fluid under pressure. Metal casings can be incorporated

---

\* The results communicated in this report were obtained in the course of an investigation conducted under Contract Nonr-225(69) by Stanford University with the Office of Naval Research, Washington, D. C. Reproduction in whole or in part is permitted for any purpose of the United States Government. This work is to be presented at the Fourth International Congress on Rheology, at Brown University, Providence, R. I., August 1963.

— a —

into the system to eliminate penetration of pressurizing fluid into the specimen and to permit more accurate strain measurement, and at the same time permit evaluation of the relaxation moduli of the polymer by means of the stress analysis theory.

## Introduction

In recent years rapid progress has been achieved in the development of methods of stress analysis for linear isotropic viscoelastic bodies within the framework of infinitesimal strain and displacement theory. For such bodies, invariance of the constitutive equations under rotation of axes implies that two independent viscoelastic operator relations are needed to prescribe the material behavior, analogous to the two independent elastic constants in classical elasticity theory. Since, for many viscoelastic bodies, shear strain magnitudes often dominate dilatational strains, it is appropriate to take as the two independent stress-strain operator relations those governing shear and dilatational deformation; for otherwise the shear behavior is likely to dominate combined operators as it does for Young's modulus for extension. The much larger deformability in shear is reflected in the literature by the much broader coverage of viscoelastic characteristics in shear and the comparative paucity of dilatational response measurements. Although measurements in shear and simple tension can formally be combined to give the separate shear and dilatational responses, practically the dilatational strain appears as the difference between two larger quantities which is therefore subject to appreciable error, and this carries over to the deduced bulk modulus characteristic functions. Direct bulk modulus measurements are difficult to carry out since the specimen must be subjected to hydrostatic pressure in a cavity, and hence the expansion of this cavity, and the compression of the pressurizing fluid must be taken into account. Moreover, the fluid may penetrate into the specimen, and small trapped air bubbles can cause major discrepancies in measurement.

Reliable response characteristics are needed for satisfactory stress analysis, and the lack of information alluded to above has hampered application of the theory, as discussed by Kolsky and Shi<sup>1</sup>, Lee<sup>2</sup>, and Hunter<sup>3</sup>. In this paper we re-assess the situation, present a method of solution for the stress distribution in a spinning pressurized circular cylinder for a material viscoelastic in dilatation, in order to indicate that analytical methods are available to treat such problems, and show how such analyses can suggest methods of measuring viscoelastic bulk characteristics.

Because of the lack of information on viscoelastic characteristics in dilatation, most treatments of viscoelastic stress analysis problems have included an assumption of uncertain validity to prescribe this property. Incompressibility<sup>4,5,6</sup> is likely to be satisfactory if the body is of open section, relatively unconfined so that free flow in shear is permitted. However, this is likely to be too drastic an assumption in many cases. Elastic dilatation<sup>5,7</sup> provides a more accurate representation. The latter introduces different operators in shear and dilatation and this can increase the complexity of certain types of analysis as mentioned below. To avoid this, the assumption has been made<sup>8,9</sup> that the operators governing shear and dilatational response differ only by a constant factor. This assumption is equivalent to the condition that the viscoelastic operator corresponding to Poisson's ratio in elasticity reduces to a constant as in elasticity, so that effectively only one time dependent operator occurs. However, as pointed out by Hunter<sup>3</sup>, there is little evidence to support this assumption, although it does provide a simple means of introducing the influence of viscoelastic response in dilatation, albeit in an artificial manner.

The analytical convenience of the assumptions mentioned above is particularly significant for analyses using differential operator stress-strain relations, since the introduction of viscoelastic compressibility would lead to higher order combined operators and hence call for more involved methods of solution. But as remarked previously<sup>10</sup>, the use of the integral operator representation of viscoelastic characteristics may not lead to appreciably more complicated analysis with viscoelastic compressibility, and further, the technique described in<sup>10</sup> allows the direct use of measured viscoelastic properties, should these be available in the appropriate form. Hence, in the following we shall incorporate, after suitable transformation, the viscoelastic dilatational characteristics given by Marvin, Adrich and Sack<sup>11</sup> into the stress analysis of a spinning, pressurized cylinder, essentially following the same procedure as that described in a previous analysis<sup>12</sup> for an elastically compressible cylinder.

#### Development of the Theory

We shall first consider the theory for plane strain, axially symmetric viscoelastic problems. Apart from the effect of the different constitutive relation for dilatation, the analysis is similar to that considered in<sup>12</sup>, in which, the material is considered to behave elastically under hydrostatic pressure. Since plane strain conditions and cylindrical symmetry are assumed, then, in conventional notation, the strains  $\epsilon_r$ ,  $\epsilon_\theta$ ,  $\epsilon_z$  and the displacement  $u$  are related by:

$$\epsilon_r = \frac{\partial u}{\partial r}, \quad \epsilon_\theta = \frac{u}{r}, \quad \epsilon_z = 0 \quad (1)$$

The stresses  $\sigma_r$ ,  $\sigma_\theta$  and  $\sigma_z$  satisfy the equilibrium equation:

$$r \frac{\partial \sigma_r}{\partial r} + \sigma_r - \sigma_\theta + \rho r^2 \omega^2 = 0 \quad (2)$$

where  $\rho$  is the mass density of the viscoelastic material, and  $\omega = \omega(t)$  is the angular velocity of rotation of the cylinder. As discussed in reference<sup>1,2</sup>, shear stress due to angular acceleration is not considered. The stresses and strains also satisfy the constitutive equations of linear viscoelasticity:

$$\sigma_r - \sigma_\theta = 2 \int_{-\infty}^t G(t-\tau) \frac{\partial}{\partial \tau} (\epsilon_r - \epsilon_\theta) d\tau \quad (3)$$

$$\sigma_r - \sigma_z = 2 \int_{-\infty}^t G(t-\tau) \frac{\partial}{\partial \tau} (\epsilon_\theta - \epsilon_z) d\tau \quad (4)$$

$$\sigma_r + \sigma_\theta + \sigma_z = 3 \int_{-\infty}^t K(t-\tau) \frac{\partial}{\partial \tau} (\epsilon_r + \epsilon_\theta + \epsilon_z) d\tau \quad (5)$$

This last equation (5) expresses the viscoelastic behavior in dilatation; a material behaving elastically in dilatation is a special case included in (5) by making the function  $K(t)$  a constant.

The material is considered undisturbed prior to zero time so that the lower limit  $-\infty$  in the integrals in (3)-(5) may be replaced by  $0^-$ . Then, just as in reference<sup>1,2</sup>, Eqs. (1)-(3) give:

$$r \frac{\partial \sigma_r}{\partial r} + \rho r^2 \omega^2 = -2 \int_{0^-}^t G(t-\tau) \frac{\partial}{\partial \tau} \left( \frac{\partial u}{\partial r} - \frac{u}{r} \right) d\tau \quad (6)$$

and hence

$$\sigma_r(r,t) = f_1(t) - \frac{1}{2}\rho r^2 \omega^2(t) - 2 \int_{0^-}^t G(t-\tau) \frac{\partial}{\partial \tau} \epsilon_\theta(r,\tau) d\tau \quad (7)$$

where  $f_1(t)$  is an arbitrary function introduced by the spatial integration. To obtain another independent equation relating  $\sigma_r$  and  $u$ , we eliminate  $\sigma_\theta$  and  $\sigma_z$  from Eqs. (3)-(5) and then use (1) to give:

$$\begin{aligned} 3\sigma_r(r,t) &= 3 \int_{0^-}^t K(t-\tau) \frac{\partial}{\partial \tau} \left( \frac{\partial u}{\partial r} + \frac{u}{r} \right) d\tau + 2 \int_{0^-}^t G(t-\tau) \frac{\partial}{\partial \tau} \left( 2 \frac{\partial u}{\partial r} - \frac{u}{r} \right) d\tau \\ &= \frac{1}{r} \int_{0^-}^t [3K(t-\tau) + G(t-\tau)] \frac{\partial^2}{\partial \tau \partial r} (ru) d\tau + 3 \int_{0^-}^t G(t-\tau) \frac{\partial}{\partial \tau} \left( \frac{\partial u}{\partial r} - \frac{u}{r} \right) d\tau \end{aligned} \quad (8)$$

In order to leave the equation with the  $u$  terms contained exclusively in a complete derivation, we use Eq. (6) to eliminate the second integral in (8), then integrate with respect to  $r$  to give:

$$\sigma_r(r,t) = \frac{f_2(t)}{r^2} - \frac{1}{4}\rho r^2 \omega^2(t) + \frac{2}{3} \int_{0^-}^t [3K(t-\tau) + G(t-\tau)] \frac{\partial}{\partial \tau} \epsilon_\theta(r,\tau) d\tau \quad (9)$$

where  $f_2(t)$  is another arbitrary function introduced by integration.

We therefore have two integral equations for the four unknown functions  $f_1(t)$ ,  $f_2(t)$ ,  $\sigma_r(r,t)$  and  $\epsilon_\theta(r,t)$ , and hence require two independent boundary conditions to properly define the problem.

In order to obtain the stress distributions it is

convenient to obtain an equation not containing displacement. This is done by operating on both sides of Eqs. (7) and (9) with the linear integral operators

$$\frac{2}{3} \int_{0^-}^t [3K(t-\tau) + G(t-\tau)] \frac{\partial}{\partial \tau} d\tau \quad \text{and} \quad 2 \int_{0^-}^t G(t-\tau) \frac{\partial}{\partial \tau} d\tau$$

respectively, and adding to give:

$$\begin{aligned} & \int_{0^-}^t [3K(t-\tau) + 4G(t-\tau)] \frac{\partial \sigma_r(r, \tau)}{\partial \tau} d\tau \\ &= \int_{0^-}^t [3K(t-\tau) + G(t-\tau)] \frac{\partial f_1(\tau)}{\partial \tau} d\tau + \frac{3}{r^2} \int_{0^-}^t G(t-\tau) \frac{\partial f_2(\tau)}{\partial \tau} d\tau \\ & \quad - \rho \frac{r^2}{4} \int_{0^-}^t [6K(t-\tau) + 5G(t-\tau)] \frac{\partial \omega^2(\tau)}{\partial \tau} d\tau \end{aligned} \quad (10)$$

This can be reduced to a much more convenient form by introducing the auxiliary function  $R(t)$  defined by the integral equation:

$$\int_{0^-}^t [3K(t-\tau) + 4G(t-\tau)] \frac{\partial R(\tau)}{\partial \tau} d\tau = 2G(t) \quad (11)$$

Then rearranging Eq. (10) so as to include all  $K$  terms only in the form  $3K + 4G$ , and using (11), linearity, and the associative property of convolutions<sup>13</sup>,  $\sigma_r(r, t)$  is given by the simpler equation:

$$\sigma_r(r,t) = f_1(t) - \frac{1}{2} \rho r^2 \omega^2(t) + \frac{3}{2} \int_0^t R(r-\tau) \frac{\partial}{\partial \tau} \left[ \frac{f_2(\tau)}{r^2} - f_1(\tau) + \frac{\rho r^2 \omega^2(\tau)}{4} \right] d\tau \quad (12)$$

which may be rewritten as:

$$\sigma_r(r,t) = F_1(t) + \frac{F_2(t)}{r^2} - F_3(t)r^2 \quad (13)$$

$$\text{where } F_1(t) = f_1(t) - \frac{3}{2} \int_0^t R(t-\tau) \frac{\partial f_1(\tau)}{\partial \tau} d\tau \quad (14a)$$

$$F_2(t) = \frac{3}{2} \int_0^t R(t-\tau) \frac{\partial f_2(\tau)}{\partial \tau} d\tau \quad (14b)$$

$$F_3(t) = \frac{\rho r^2}{8} [4\omega^2(t) - 3 \int_0^t R(t-\tau) \frac{\partial \omega^2(\tau)}{\partial \tau} d\tau] \quad (14c)$$

using (13) and (2),  $\sigma_\theta$  is given by:

$$\sigma_\theta(r,t) = F_1(t) - \frac{F_2(t)}{r^2} + [3F_3(t) + \rho \omega^2(t)]r^2 \quad (15)$$

For the non-rotating cylinder ( $\omega=0$ ) Eqs. (13) and (15) are immediately recognized as the Lamé solution, which is independent of material properties if the two independent boundary conditions specify the surface tractions. For the more general rotating case (14c) gives  $F_3(t)$  and knowledge of the internal and external pressures then immediately determines  $F_1(t)$  and  $F_2(t)$  and hence the

stress distributions. If, however, one or both surfaces has a bonded elastic casing, the stress solution is not so simple. At such a surface, the boundary condition relates the normal stress to the displacement<sup>14</sup> according to:

$$\sigma_r(b,t) = -B \epsilon_\theta(b,t) \quad (16)$$

where  $b$  is the boundary radius, and

$$\frac{1}{B} = \frac{1 + \nu_b h(1 - \nu_b^2)}{E_b(1 + \nu_b)} \quad (17)$$

where  $E_b$ ,  $\nu_b$  and  $h$  are the Young's modulus, Poisson's ratio and thickness respectively of the reinforcing elastic casing.

If only one surface has a bonded elastic casing, and the other has prescribed normal pressure, the method of solution is precisely that described in reference<sup>12</sup> with the R-function now defined by (11). The method involves using the pressure boundary condition

$$\sigma_r(a,t) = -p_a(t) \quad (18)$$

and the casing boundary condition (16) together with (7) for  $r = b$ , and (12) for  $r = a, b$  to eliminate  $f_2(t)$  and obtain two interrelated convolution integral equations for  $\sigma_r(b,t)$  and  $f_1(t)$ , which can be simultaneously solved numerically by finite difference techniques.  $\sigma_r(r,t)$  and  $\sigma_\theta(r,t)$  are then immediately given by Eqs. (13) and (15).

If both boundary conditions are of the casing type (16), then both can be applied to each of Eqs. (7) and (9)

permitting elimination of  $f_1(t)$  and  $f_2(t)$  and hence again obtain two interrelated convolution integral equations, but this time for  $\sigma_r(a,t)$  and  $\sigma_r(b,t)$  (or the equivalent boundary strains). Either  $f_1(t)$  or  $f_2(t)$  are then given by simple quadratures, and substitution in Eqs. (13) and (15) determines  $\sigma_r(r,t)$  and  $\sigma_\theta(r,t)$ .

So far we have only considered the determination of the stress distributions. Obtaining the displacement field would seem to involve only a simple choice between, solving the integral equations (7) or (9) for  $\epsilon_\theta(r,t)$  and hence  $u(r,t)$ . Of these two equations, (7) seems to be the preferable since it may be rewritten in the quadrature form:

$$\epsilon_\theta(r,t) = \frac{1}{2} \int_0^t J(t-\tau) \frac{\partial}{\partial \tau} [f_1(\tau) - \frac{1}{2} \rho r^2 \omega^2(\tau) - \sigma_r(r,\tau)] d\tau \quad (19)$$

where  $J(t)$  is the creep compliance, either a measured material characteristic or determined from  $G(t)$  as by Hopkins and Hamming<sup>15</sup>. However, in order to achieve satisfactory numerical accuracy, Eq. (9) is in fact to be preferred and when rewritten in the form:

$$\int_0^t [3K(t-\tau) + G(t-\tau)] \frac{\partial}{\partial \tau} [b^2 \epsilon_\theta(b,\tau) - r^2 \epsilon_\theta(r,\tau)] d\tau = \frac{3}{2} [b^2 \sigma_r(b,t) - r^2 \sigma_r(r,t)] + \frac{3}{8} (b^4 - r^4) \rho \omega^2(t) \quad (20)$$

it may be solved as a Volterra integral equation for  $\epsilon_\theta(r,t)$ . Another equation for  $\epsilon_\theta(r,t)$ , not containing  $G(t)$  directly, may be obtained by eliminating the  $G$  term from Eq. (7) and (9), and  $f_2(t)$  through the substitution  $r = b$ , to give:

$$\int_0^t 6K(t-\tau) \frac{\partial}{\partial \tau} [b^2 \epsilon_{\theta}(b, \tau) - r^2 \epsilon_{\theta}(r, \tau)] d\tau = b^2 [4\sigma_r(b, t) - f_1(t)] - r^2 [4\sigma_r(r, t) - f_1(t)] \quad (21)$$

This equation is more suitable for the determination of displacements for elastically compressible materials since it then reduces to a simple algebraic expression for  $\epsilon_{\theta}(r, t)$ .

#### Particular Example

The particular example to be considered in this section is that of a hollow cylinder of polyisobutylene encased in an elastic shell and subjected to arbitrary internal pressure. Although in the numerical example presented later the cylinder is non-rotating and non-ablating, the theory developed in the previous section, and the method of numerical evaluation used, apply for the general case.

The choice of material and loading conditions was governed by the availability in the literature of measured physical characteristics in shear and dilatation. Marvin, Aldrich and Sack<sup>11</sup> give complex shear and bulk moduli for polyisobutylene over an equivalent frequency range of  $10^6$  to  $10^9$  cycles/sec. when the measurements are reduced to 25°C. Although these cannot be substituted directly into the theory presented here, which is based on relaxation moduli, in the absence of measurements of the latter, we decided to base the solution on the relaxation moduli deduced approximately from the complex modulus measurements, since our objective was to present an example illustrative of the method which might serve to encourage more precise measurements of viscoelastic

dilatational characteristics to permit application of this approach. We therefore used the empirical formulae proposed by Ninomiya and Ferry<sup>16</sup> for evaluating approximate relaxation moduli:

$$G(t) = G'(\omega) - 0.40 G''(0.40\omega) + 0.014 G''(10\omega) \Big|_{\omega = 1/t} \quad (22a)$$

$$K(t) = K'(\omega) - 0.40 K''(0.40\omega) + 0.014 K''(10\omega) \Big|_{\omega = 1/t} \quad (22b)$$

Fig. 1 shows the resulting moduli plotted logarithmically, the experimental results having been smoothed by differencing. Because of the equivalent high frequency at the reduced temperature of 25°C, direct evaluation of the relaxation moduli by (22) would cover a time range in micro-seconds, which would be unsuitable for the quasi-static stress analysis problem under consideration. We therefore consider pressurizing to occur at a lower temperature which introduces a factor of 10<sup>4</sup> in the time scale on the basis of the thermo-rheologically simple hypothesis<sup>17</sup>. This corresponds to a temperature of about -55°C, at which quasi-static analysis would be satisfactory for loading times in the range of the relaxation data. The time scale in Fig. 1, and the example to be presented, correspond to this temperature, although the solution can be interpreted to correspond to different loading times at different temperatures, as long as the temperature is not considered raised to the extent that inertia forces due to the deformation become significant. It is seen from Fig. 1 that much more marked relaxation occurs in shear than in dilatation, but that the latter occurs sooner.

R(t) was obtained from the integral equation (11) by finite sum numerical evaluation as described in reference<sup>10</sup>. Fig. 2 shows the variation of R(t)

computed using several step lengths. It is evident that practical convergence is achieved for  $\Delta(\log t) = 0.0625$ . For comparison the corresponding curves for elastically compressible bodies are shown, assuming the constant bulk modulus to coincide with the initial modulus,  $K(0)$ , and long-time modulus,  $K(\infty)$ , respectively. Comparison of the influence of the time step  $\Delta(\log t)$  with that for the elastically compressible case<sup>10</sup> reveals much slower convergence for viscoelastic dilatation. Whereas in the elastically compressible case  $R(t)$  is monotonically decreasing, Fig. 2 shows this to be no longer so. That this behavior is permissible is clear from a physical interpretation of the meaning of the function.

$R(t)$  defined by (11) is a generalization of the  $R$  function introduced by Muki and Sternberg<sup>7</sup>. It has a physical interpretation in terms of one-dimensional strain with displacement parallel to the  $x_1$  axis and independent of the  $x_2, x_3$  coordinates. The principal strains are then  $(\epsilon_1, 0, 0)$  and stresses  $(\sigma_1, \sigma_2, \sigma_2)$ , and the linear viscoelastic laws in shear and dilatation give:

$$\sigma_1(t) - \sigma_2(t) = \int_{-\infty}^t 2 G(t-\tau) \frac{\partial \epsilon_1}{\partial \tau} d\tau \quad (23a)$$

$$\sigma_1(t) + 2\sigma_2(t) = \int_{-\infty}^t 3K(t-\tau) \frac{\partial \epsilon_1}{\partial \tau} d\tau \quad (23b)$$

Elimination of  $\sigma_2$  yields:

$$3\sigma_1(t) = \int_{-\infty}^t [3K(t-\tau) + 4G(t-\tau)] \frac{\partial \epsilon_1}{\partial \tau} dt \quad (24)$$

Comparison with (11) shows  $R(t)$  to be the strain response  $\epsilon_1(t)$  with this one-dimensional constraint for a stress variation  $2G(t)/3$ , and hence  $\epsilon_1(t)$  can increase with time as does creep response.

In the previous section we showed that for a cavity of radius  $a$  subjected to pressure  $p(t)$ , with an elastic casing at  $r = b$ , a pair of integral equations for  $\sigma_r(b,t)$  and  $f_1(t)$  can be deduced for (7) and (12). Transformed into a convenient form for numerical analysis they reduce to the equations given in reference<sup>12</sup> for the elastically compressible case, modified to accommodate the minor change in the definition of  $R$ :

$$\left[1 - \frac{2}{B} G(0)\right] \sigma_r(b,t) + \frac{2}{B} \int_0^t \sigma_r(b,\tau) \frac{\partial}{\partial \tau} G(t-\tau) d\tau = f_1(t) - \frac{1}{2} p r^2 \omega^2(t) \quad (25a)$$

$$\begin{aligned} & \left[1 - \frac{3}{2} R(0)\right] f_1(t) + \frac{3}{2} \int_0^t f_1(\tau) \frac{\partial}{\partial \tau} R(t-\tau) d\tau \\ & = \frac{1}{b^2 - a^2} [b^2 \sigma_r(b,t) + a^2 p(t) + (b^4 - a^4) F_3(t)] \quad (25b) \end{aligned}$$

As described in reference<sup>12</sup> these can be solved conveniently by finite sum approximation, in a manner similar to that for single integral equations<sup>10</sup>. Programming was carried out in the computer language BALGOL, for processing on the IBM 7090 machine at the Stanford University Computing Center. These facilities were in part made available under the National Science Foundation Grant NSF-GP 948.

In order to have an appreciable influence of viscoelasticity in dilatation, Fig. 1 shows that a loading

time of the order  $10^{-3}$  secs. is needed, and so the pressure variation in the cavity was taken to be:

$$p(t) = p_{\infty}(1 - e^{-1000t}) \quad (26)$$

Since the stiffness of the external elastic casing is likely to have a significant influence on the stress distributions<sup>12</sup>, the solution was carried out for a "soft" casing,  $B = 1.434 G(0)$ , which corresponds to an aluminum casing with  $b/h \sim 150$ , a "medium" casing,  $B = 3.441 G(0)$ , which corresponds to a steel casing with  $b/h \sim 80$ , and for a rigid casing.

Table I shows the dimensionless compressive stress values ( $\sigma/p_{\infty}$ ) for various times and boundary positions for the medium casing, compared with the corresponding problems with elastic compressibility and  $K = K(0)$  and  $K(\infty)$  respectively. Because of the rapid initial variation, equal steps of  $\log t$  were taken for the finite sum approximation for  $t < 0.01$ , and equal steps of  $t$  thereafter. The steps were halved until a difference of less than  $\frac{1}{2}\%$  in  $\sigma_r$  resulted, this occurring for the viscoelastic case with  $\Delta(\log t) = 0.125$  and  $\Delta t = 0.005$ . The results in Table I show that for the longer times the elastically compressible solution with  $K = K(\infty)$  provides a good approximation for both stress components, as would be expected from the form of the relaxation modulus in dilatation shown in Fig. 1. Viscoelasticity in dilatation influences the  $\sigma_{\theta}$  component appreciably at the shortest time, and particularly the value of  $\sigma_{\theta}(a,t)$ . At the later times, the dominating relaxation in shear leads to almost hydrostatic stress conditions with the two stress components almost equal.

For the softer casing larger displacements occur, with

consequent larger stress differences, and for the same time steps the effect of halving the step length produced a change of about 2% in  $\sigma_r$ , showing somewhat larger, though acceptable, truncation errors.

It was pointed out at the end of the previous section that displacements could be evaluated from the inversion of (7) in the form (19) which depend on the viscoelastic shear operator, or by (20) which contains an operator dominated by the dilatational viscoelastic kernel  $K(t)$  (since as shown in Fig. 1,  $K(t) \gg G(t)$ ). For an encased cylinder, after the initial rapid growth of displacement, continued expansion is inhibited by the casing and the dilatational material characteristics, and shear restraint virtually disappears as the stress-differences relax. Thus when using (19) the constraining effect must arise since  $f_1(\tau) - \frac{1}{2}pr^2\omega^2 - \sigma_r(r,\tau) \sim 0$ . In the example considered here,  $\omega = 0$ , and the computation of the displacement then depends on the difference of two nearly equal computed quantities. This leads to considerable numerical error, and as shown by the points plotted in Fig. 3 for  $\epsilon_\theta(a,t) = u/a$  for the medium casing,  $B = 3.441 G(0)$ , satisfactory convergence was not achieved even for time increments one quarter those used for the stress calculations. Use of (20), in which the constraint on  $u$  is introduced in a natural way through the dilatational operator, no such difficulty arose and the change in  $u$  for halving the time step for the courser increments used for the stress calculations was less than 1%.

Fig. 3 shows the circumferential strain at the cavity surface,  $\epsilon_\theta(a,t) = u(a,t)/a$ , thus being a measure of displacement, for the two elastic casings mentioned above, and for a rigid casing. Values calculated for elastic compressibility, for  $K(0)$  and  $K(\infty)$ , are also shown.

In Fig. 3  $\epsilon_{\theta}$  is presented in dimensionless form  $\bar{\epsilon}_{\theta} = G(0) \frac{\epsilon_{\theta}}{p_{\infty}}$  which accounts for the magnitude of order unity. It is evident that the stiffness of the casing has a major effect on the displacements, and that with increasing time the displacement for the body exhibiting viscoelasticity in dilatation approaches the elastically compressible case with  $K = K(\infty)$ . This would be expected in view of the  $K(t)$  variation shown in Fig. 1, and the influence of dilatational constraint in this problem. The approach however is slow, and in fact the limit would only be achieved when a hydrostatic stress condition has developed. Table I shows that this has not been achieved at  $t = 0.1$  since  $(\sigma_r - \sigma_{\theta})$  is still appreciable, and  $\sigma_z$  can be expected to differ by an amount of the same order. Only when the maximum shear stresses, i.e. the stress differences, have relaxed to zero, will elastic dilatational constraint based on  $K(\infty)$  determine the displacement correctly.

For the rigid casing example, incompressible material behavior would give  $u \equiv 0$ , and we see that the elastically compressible case based on  $K(0)$  is closer to this result than to the dilatational viscoelastic and  $K(\infty)$  cases. For  $K(0)$ , the Poisson's Ratio of instantaneous response is 0.43, compared with 0.27 for  $K(\infty)$ . It is thus clear why the former, with growth towards 0.5 as the shear modulus relaxes, is close to the incompressible solution.

The results discussed above indicate that in this problem dilatational viscoelasticity has overall only a moderate influence on the stress and displacement distributions. If such a configuration were envisaged for measuring dilatational properties, therefore, facilities for accurate measurements of surface displacement would be needed. This consideration is assessed in the following section.

### Application for Measuring Dilatational Characteristics

The analyses given above to determine stresses and displacements for materials exhibiting viscoelasticity in dilatation as well as in shear, can be used in reverse to determine the relaxation moduli in shear and dilatation from displacement measurements. However, the comparative stiffness in dilatation calls for extremely accurate displacement measurements to achieve satisfactory dilatational modulus values. Measurement of surface displacements or strains for viscoelastic bodies is hampered by the texture of many polymeric specimens which have a geometrically less smoothly defined surface than for structural metals, and which are often too soft compared with resistance strain gauge elements, or modified by glue used for attaching them, to permit sufficient accuracy of measurement. If a cylindrical specimen can be reinforced, both internally and externally, by elastic metal casings, accurate displacement measurements could be made on the metal surfaces, following internal pressure or spin, and the analysis given above can be transformed for the determination of  $G(t)$  and  $K(t)$ .

For example, if we consider the internal and external shell constants (17) to be  $B_a$  and  $B_b$  respectively, and consider expansion due to spin only, equation (20) can be expressed in the form

$$\int_0^t L(t-\tau) \frac{\partial X(\tau)}{\partial \tau} d\tau = Y(t) \quad (27)$$

where  $L(t) = 3K(t) + G(t)$

$$X(t) = b u(b,t) - a u(a,t)$$

$$Y(t) = - 3[b B_b u(b,t) - a B_a u(a,t)] / 2 + 3(b^4 - a^4) \rho \omega^2(t) / 8$$

and equation (7) in the form:

$$2 \int_0^t G(t-\tau) \frac{\partial U(\tau)}{\partial \tau} = V(t) \quad (28)$$

where  $U(t) = u(b,t)/b - u(a,t)/a$

$$V(t) = - B_b u(b,t)/b - B_a u(a,t)/a - \rho \omega^2(t)(b^2 - a^2)/2$$

For measured  $u(b,t)$  and  $u(a,t)$ , (27) and (28) can be solved numerically for  $L(t)$  and  $G(t)$  just as (11) was solved for  $R(t)$ <sup>10</sup>.  $K(t)$  then follows from:

$$K(t) = [L(t) - G(t)]/3 \quad (29)$$

Measurements of the displacement on steel or aluminum rings, for example, may prove sufficiently accurate to permit satisfactory evaluation of  $K(t)$ .

Similar approaches can be adopted for other loading situations which may be more convenient experimentally than the above suggestion based solely on centrifugal inertial loading. This was chosen for illustrative purposes to permit direct application of equations already developed in this paper. Eqs. (16) and (17) can be readily modified to include internal pressure on the inner ring, as well as support pressure at the metal-plastic interface, so that a similar integral equation for the evaluation of  $K(t)$  follows from displacement measurements following application of a known internal pressure variation. Such a configuration would have the advantage of maintaining pressure at the metal-plastic interfaces and hence avoid adhesion problems. Alternatively, for known internal pressure without an inner ring, measurements of the

displacement of the outer casing could be used to determine  $K(t)$ , if  $G(t)$  were measured independently, for example by measurements of torsion. Since the method of evaluation is numerical solution of integral equations, direct computation from experimental readings of displacement or pressure is available.

A similar but simpler analysis can be carried out for the spherically symmetrical problem, simpler since only two independent principal stress components need be considered in the theory ( $\sigma_r, \sigma_\theta, \sigma_\theta$ ) compared with three in the cylindrical case. However, the construction of spherical specimens with well fitting elastic casings is likely to present extremely difficult problems of fabrication, and hence it seems unlikely that this approach will lead to applications. The analysis is therefore not presented.

### Bibliography

1. H. Kolsky and Y. Y. Shi, "The validity of model representation for linear viscoelastic behavior," Brown University Report Nonr 562(14)/5 (1958).
2. E. H. Lee, "Viscoelastic stress analysis", Proceedings First Symposium on Naval Structural Mechanics, Pergamon Press, Oxford (1960).
3. S. C. Hunter, "Viscoelastic Waves", Progress in Solid Mechanics, 1 (1960).
4. T. Alfrey, Quart. Appl. Math., 2, 113 (1944).
5. E. H. Lee, J. R. M. Radok and W. B. Woodward, Trans. Soc. Rheol., 3, 41 (1959).
6. M. Shinozuka, "Stresses in a linear incompressible viscoelastic cylinder with moving inner boundary, ASME Paper No. 63-APMW-2 (1963).
7. R. Muki and E. Sternberg, J. Appl. Mech., 28, 193 (1961).
8. H. S. Tsien, Quart Appl. Math., 8, 104 (1950).
9. C. C. Chao and J. D. Achenbach, "Stress waves in a viscoelastic solid," to appear in the Proc. IUTAM Symp. on Anelastic Waves, Brown University (1963)
10. E. H. Lee and T. G. Rogers, Jl. Appl. Mech. 30, 127 (1963).
11. R. S. Marvin, R. Aldrich and H. S. Sack, J. Appl. Phys., 25, 1213 (1954).
12. T. G. Rogers and E. H. Lee, "The cylinder problem in viscoelastic stress analysis," Technical Report No. 138, Division of Engineering Mechanics, Stanford Univ., (1963); to appear in Quart. Appl. Math.
13. F. G. Tricomi, "Integral Equations", Interscience Publishers Inc., New York (1957).
14. L. W. Morland and E. H. Lee, Trans. Soc. Rheol. 4 233 (1960).
15. I. L. Hopkins and R. W. Hamming, J. Appl. Phys. 28, 906 (1957).

Bibliography (Con't)

16. K. Ninomiya and J. D. Ferry, J. Colloid Sci. 14,  
36 (1959).
17. F. Schwarzl and A. J. Staverman, J. Appl. Phys, 23  
838 (1952).

Table I Compressive Stress Values

$$[\sigma_r(a,t) = 1 - e^{-1000 t}]$$

|                      |               | t → | 0.001 | 0.01  | 0.1   |
|----------------------|---------------|-----|-------|-------|-------|
| $\sigma_r(b,t)$      | K(0)          |     | .489  | .949  | .991  |
|                      | K(t)          |     | .460  | .920  | .986  |
|                      | K( $\infty$ ) |     | .452  | .918  | .986  |
| $\sigma_\theta(b,t)$ | K(0)          |     | .260  | .867  | .978  |
|                      | K(t)          |     | .207  | .792  | .962  |
|                      | K( $\infty$ ) |     | .163  | .788  | .964  |
| $\sigma_r(a,t)$      | all K         |     | .632  | 1.000 | 1.000 |
| $\sigma_\theta(a,t)$ | K(0)          |     | .118  | .817  | .969  |
|                      | K(t)          |     | .043  | .712  | .948  |
|                      | K( $\infty$ ) |     | .018  | .673  | .950  |

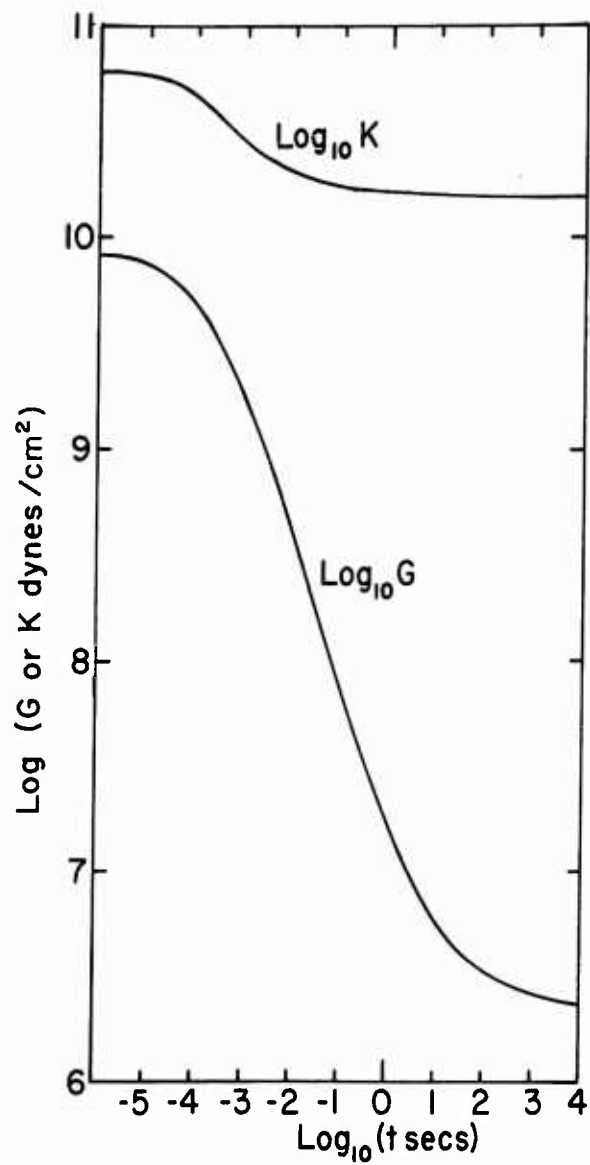


Fig.1 Relaxation Moduli of Polyisobutylene  
in Dilatation (K) and Shear (G)

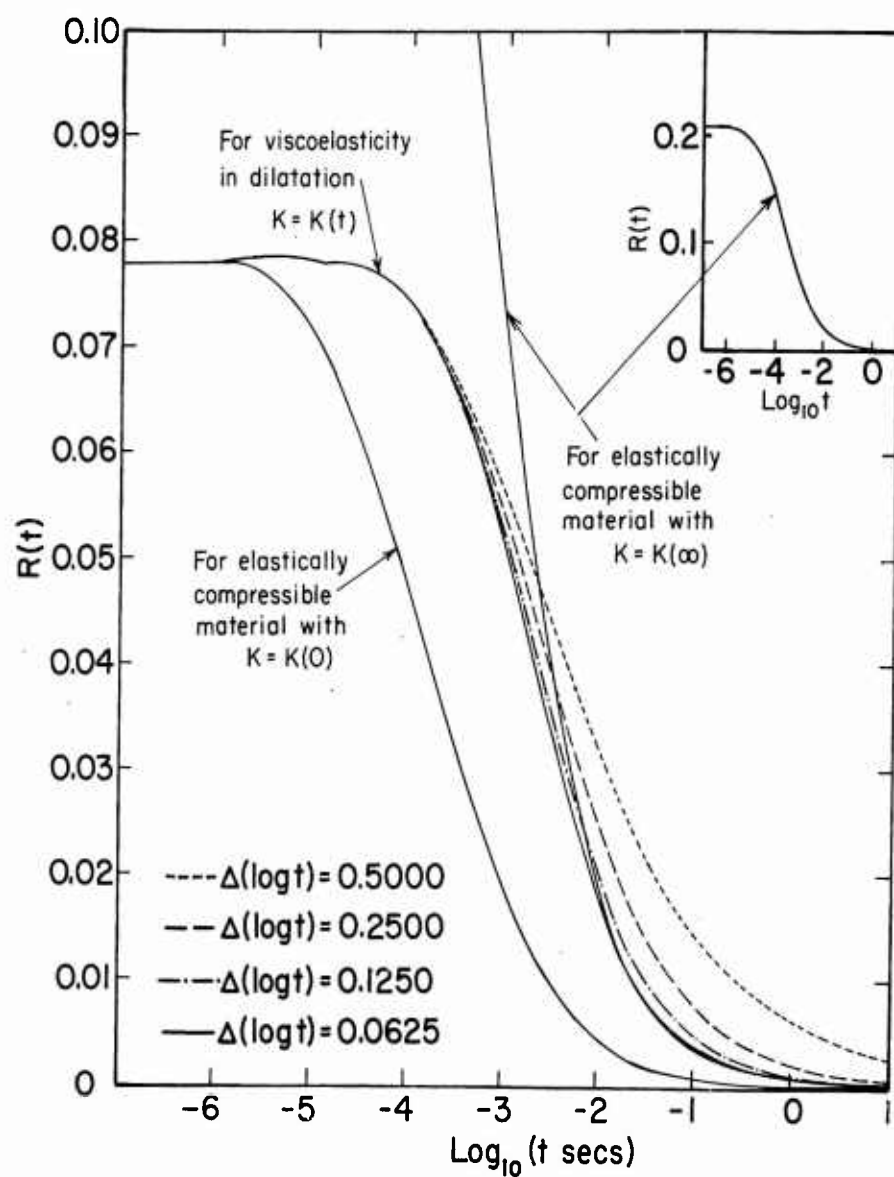


Fig. 2 Characteristic Functions  $R(t)$  for Polyisobutylene

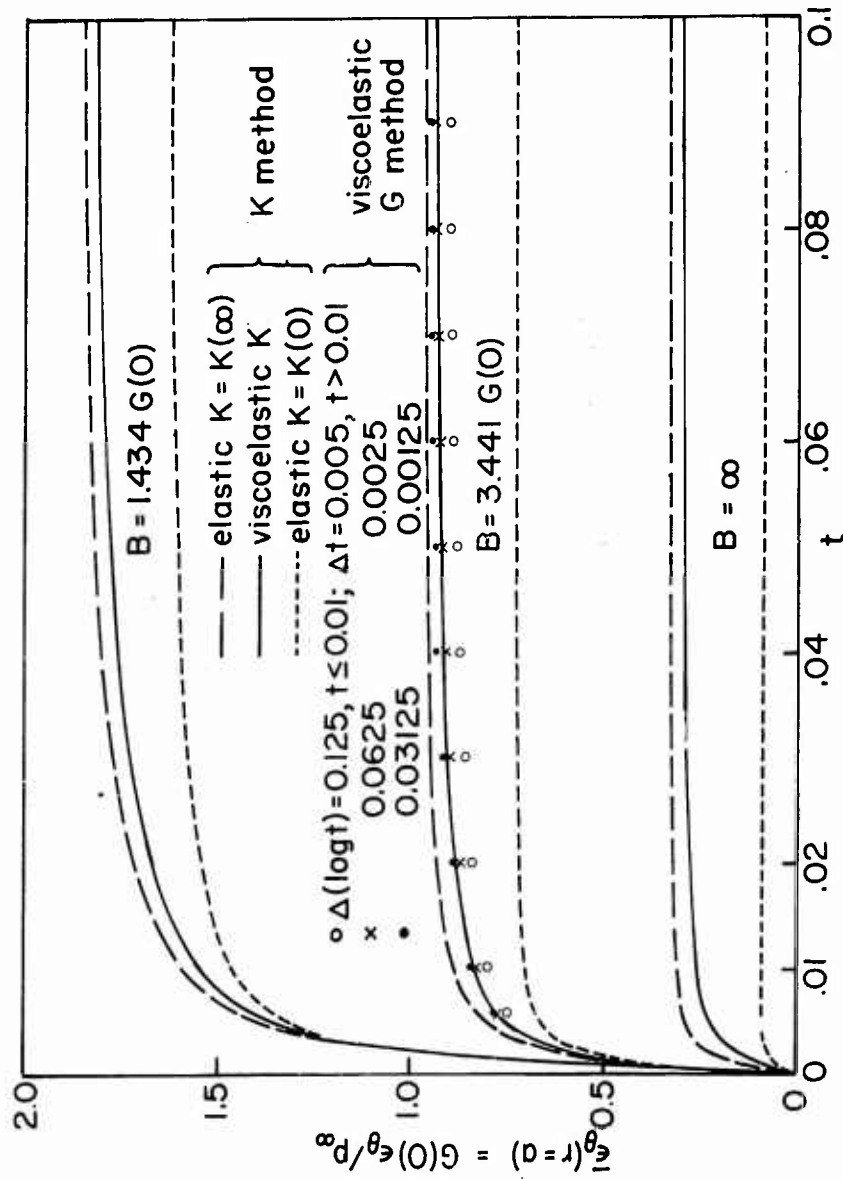


Fig. 3 Variations of the Internal Boundary Displacements for different Compressibilities and elastic casings